Determining the ion velocity in the inner magnetosphere of comet 67P/Churyumov-Gerasimenko using Rosetta IES measurements

EGU2020-3347

Z. Nemeth*, K. Szego, A. Timar, L. Foldy, J. Burch, R. Goldstein

*nemeth.zoltan@wigner.hu

- **Aim:** To determine an upper limit for the bulk speed of the plasma ions in the innermost region of the cometary magnetosphere (inside and near the diamagnetic cavity).
- **Method:** We compared the angular and energy distributions of the plasma ions measured on 25-27 and 29-31 July 2015 with simulated distributions taking into account the effects of the spacecraft potential.
- **Results:** The thermal speed of the ions is less than 3.5 km/s, their bulk speed is less than 2 km/s. This is an upper limit, the actual speeds can be significantly less.

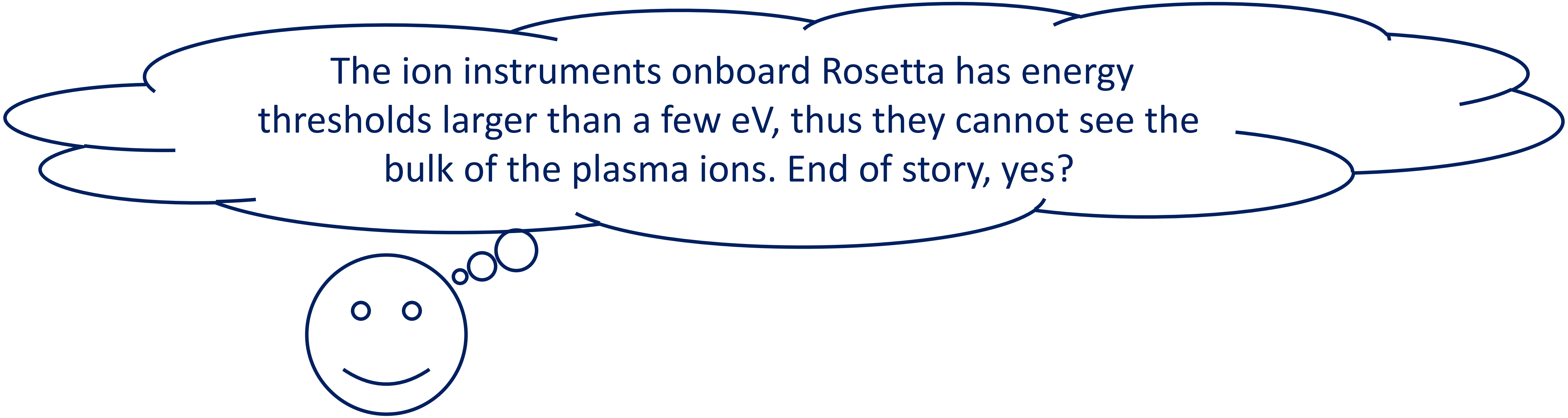

- **Most definitely not!**
- Most of the time the spacecraft potential is negative, usually between -5V and -25V (Odelstad et al., 2017; Stenberg Wieser et al., 2017)
- Such a potential will accelerate the ions to energies over the instrument threshold and bend the trajectories (Goldstein et al. 2015, Bergman et al. 2020)
- The angle and energy distribution of the ions entering the instrument contain information about the original velocity distribution.

How the properties of the original velocity distribution influence the measurements?

- A nonzero bulk speed causes anisotropy
- The higher the temperature the lower the apparent anisotropy for the same bulk speed
- The effects of the spacecraft potential (U_{SC}) also lessen the anisotropy (bent trajectories)

⇩

- From the measured anisotropy we can determine the ratio of the bulk and thermal speeds

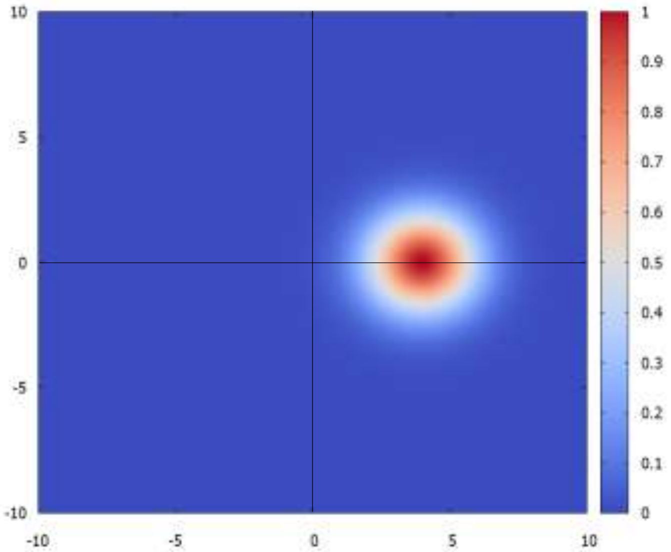

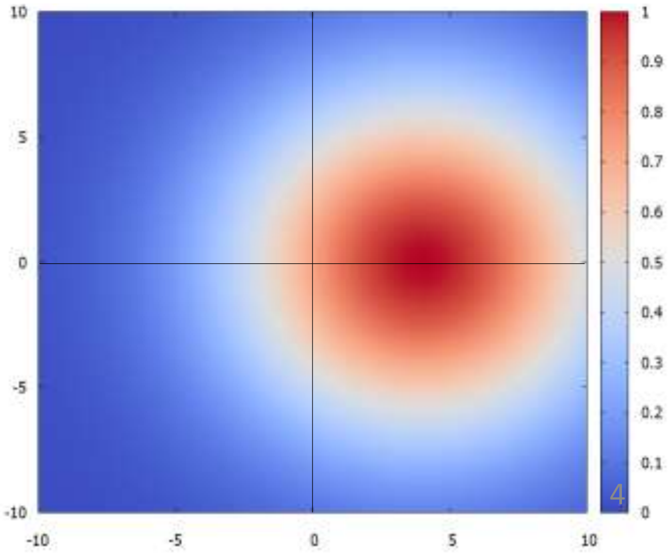

How the properties of the original velocity distribution influence the measurements?

- Higher bulk speed shifts the energy distribution upward
- Higher temperature expands the width of the distribution → even higher max speeds, lower min speeds
- Negative U_{SC} shifts the distribution upward
- Caveat:

If a significant portion of the distribution is below the instrument threshold, the measured anisotropy and bulk speed can be higher than reality

Simulated energy spectrum, USC=-30V

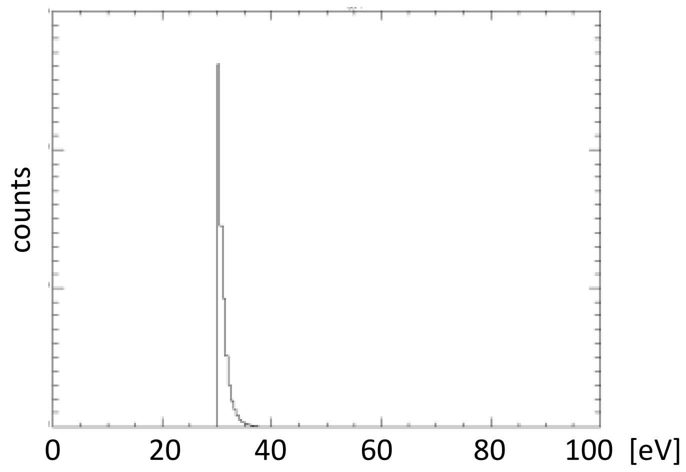

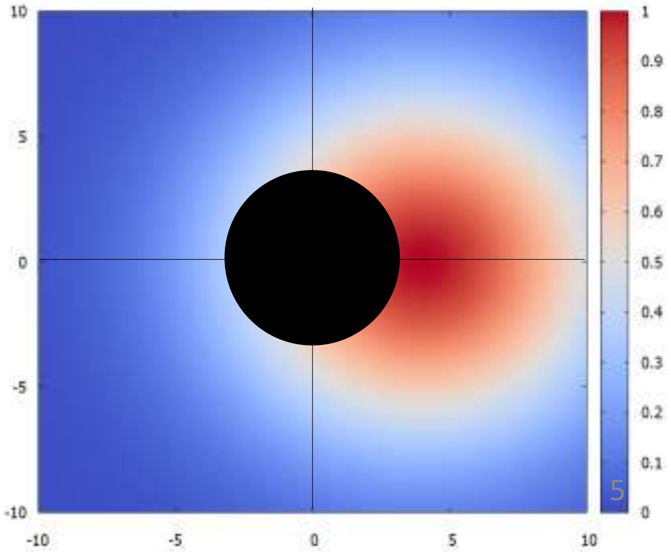

Simulations

- We simulated the effects of the spacecraft potential by following the motion of test particles having a shifted Gaussian initial distribution in the potential of a spherical spacecraft.
- Each simulation run had three parameters: the bulk and thermal speeds and U_{SC}
- We computed the final energy and angular distribution of the ions entering the instrument

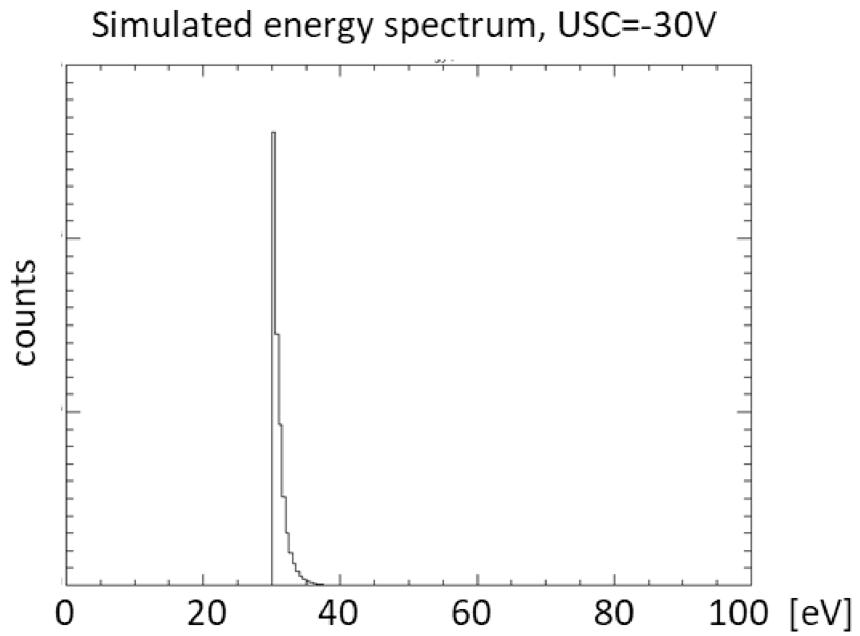

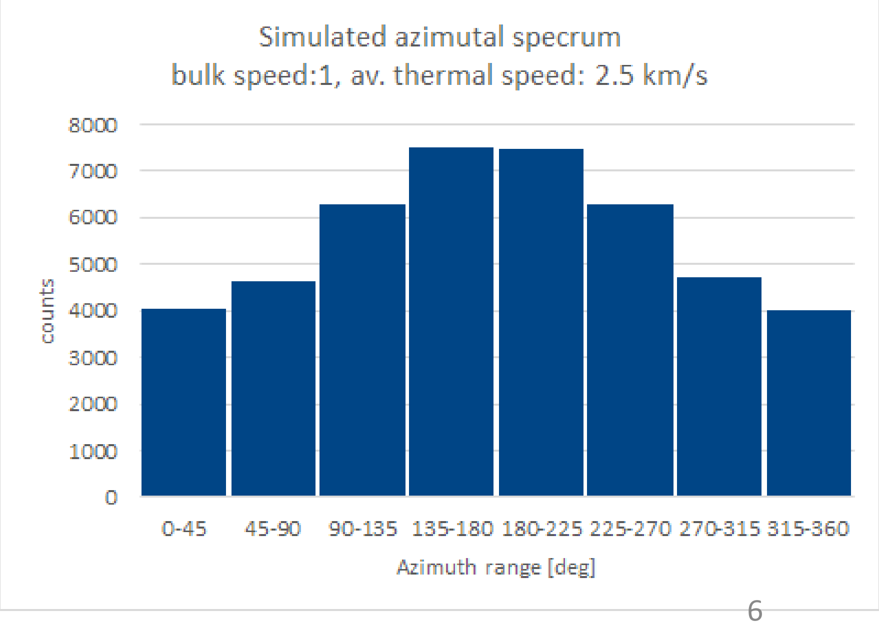

Angular distribution

- The measured and simulated angular distributions can be compared directly by comparing the shapes of the distributions (the width of the peaks)
- We can determine plausible bulk speed – average thermal speed pairs.
- A few possible pairs are shown in the table in km/s units
- The plasma is warm: $v_{th} \geq v_b$
- The v_{th}/v_b ratio increases with v_b

Bulk speed	Thermal speed
1	1
1	1.25
1	1.5
1.5	1.875
1.5	2.25
1.5	2.625
2	3
2	3.5
2.5	3.75
2.5	4.375
2.5	5
3	5.25
3	6
3.5	6.125
3.5	7
4	7

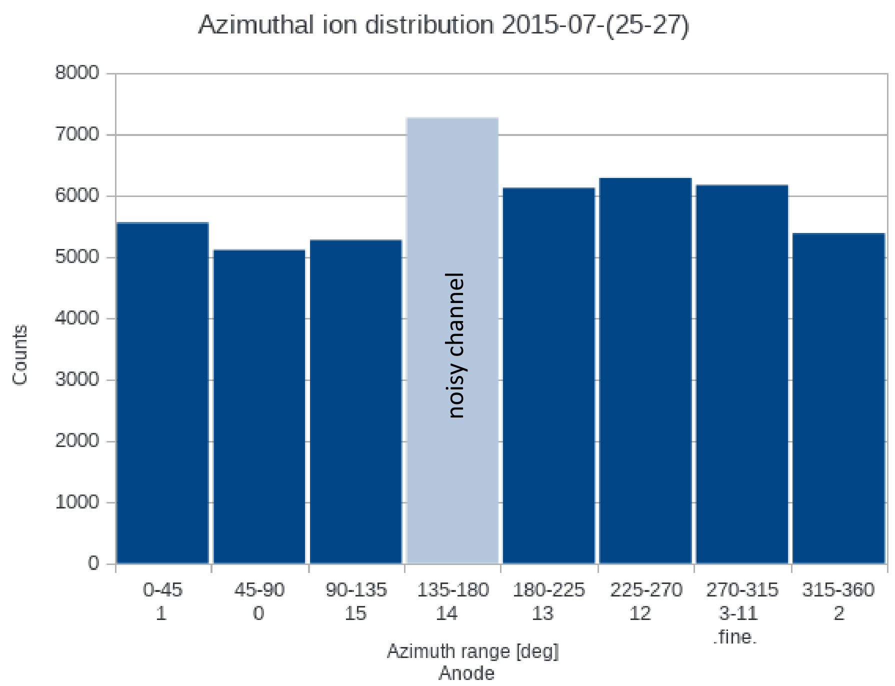

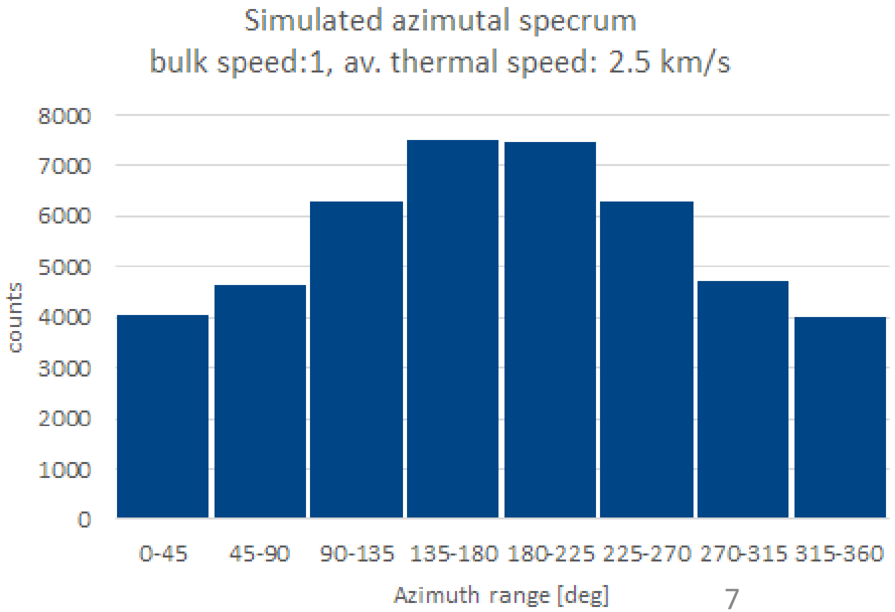

Energy distribution

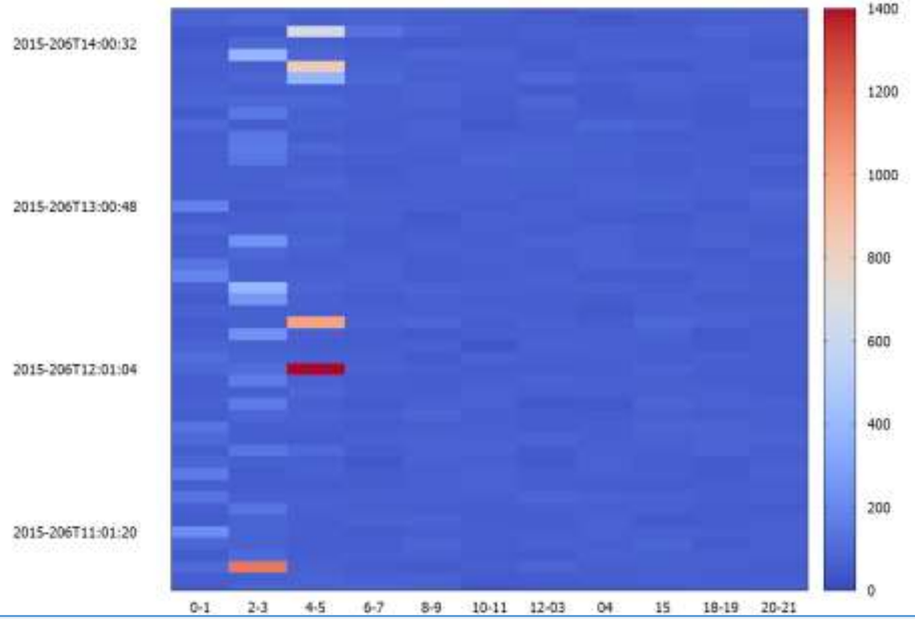

- Due to telemetry limitations the energy resolution of low energy IES data is 8.6 eV in these time intervals

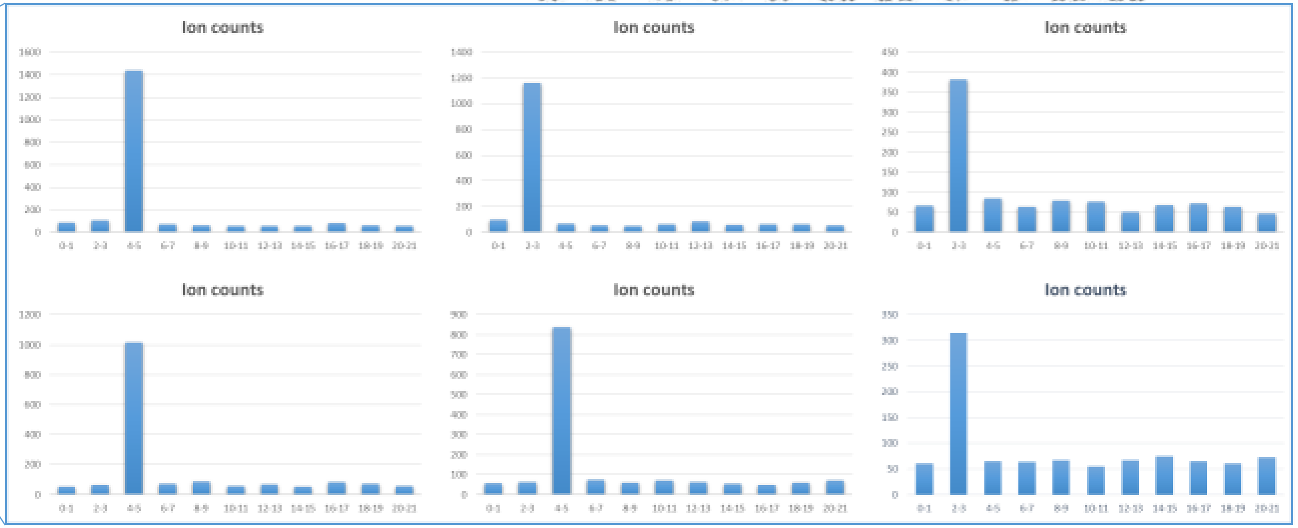

- 8.6 eV is quite large for bulk plasma ions, thus most of their spectrum contribute only to a single energy bin

- If the value of $q \cdot U_{SC}$ is close to the energy bin boundary, some of the spectrum falls into the next bin – hence we have two bin measurements as well

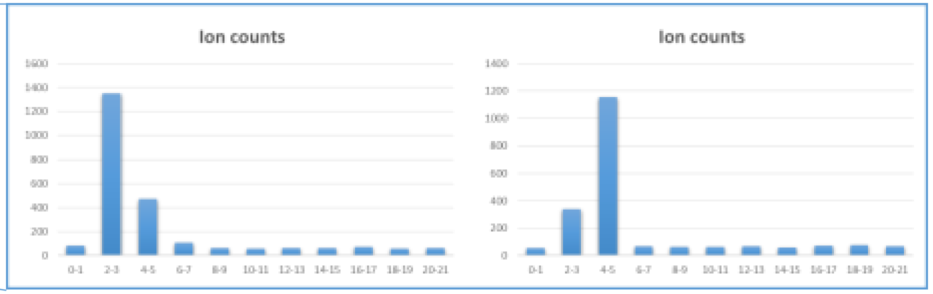

Energy distribution

- The spacecraft potential changes rapidly, it can change more than 10 V between consecutive measurements (as measured by the LAP instrument)
- In such cases the energy spectrum suffers a corresponding rapid shift during a single ion measurement – thus (rarely) the corresponding ion counts can appear in three adjacent energy bins

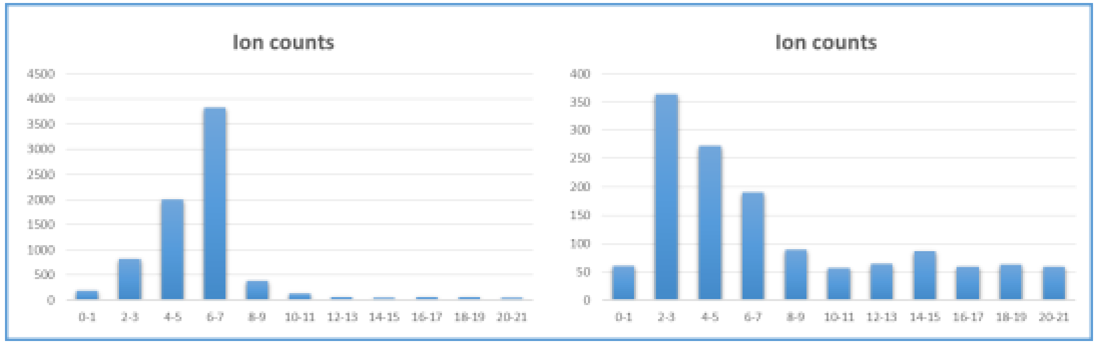

Energy distribution

- The simulated energy spectrum of the ions entering the instrument feature a rapid rise near U_{SC}, and a nearly exponential fall-off after the peak
- It is easy to calculate how many of the counts would fall into a single bin for a given value of U_{SC}
- The single-bin peaks most common in the data suggest that the characteristic energy scale of the exponential fall-off is significantly smaller than the bin size (in the opposite case the peak would extend to several energy bins)
- Due to a fluctuating background the contribution of the spectrum to the other bins is difficult to measure for smaller peaks. Using the most prominent peaks we can see that it is less than 1%
- From this we can determine an upper limit for the characteristic energy scale of the exponential fall-off (E_0):
- $E_0 < 2$ eV
- Note: Due to the rapid variation of U_{SC} the time-integrated energy spectrum cannot be used to recover the fine details of the original energy spectrum

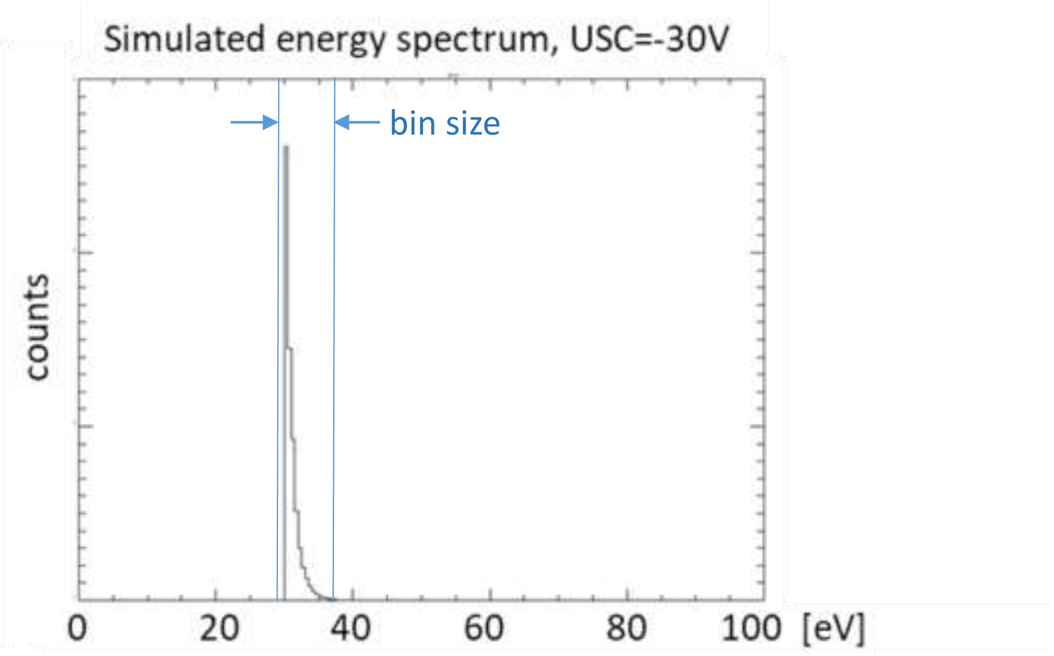

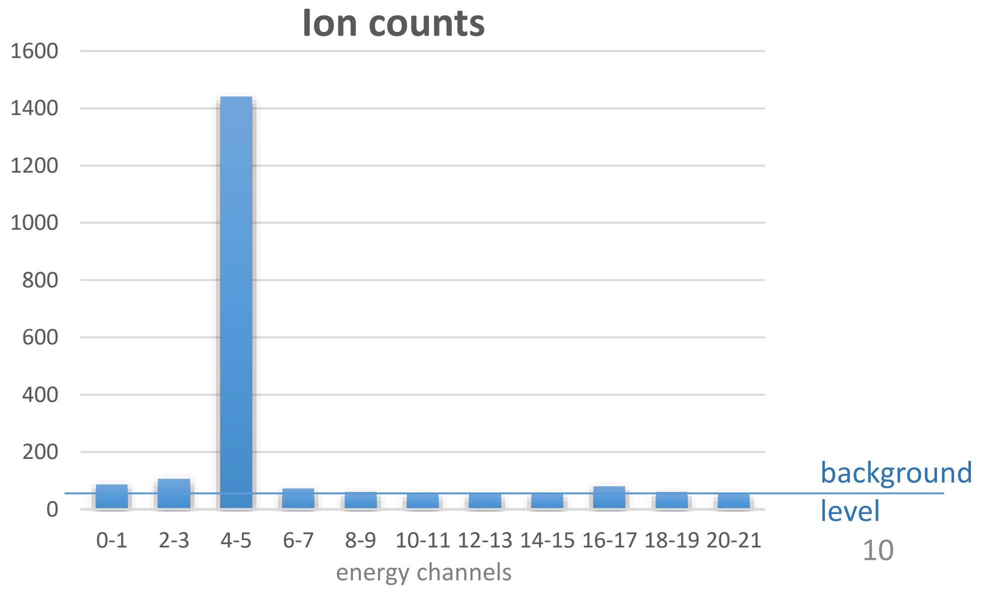

Constraints

- Using the measured angular distribution we can determine a constraint for the v_{th}/v_b ratio
- The plasma is warm ($v_{th}/v_b > 1$)
- The v_{th}/v_b ratio increases with the bulk speed
- From the simulated energy spectrum we can compute the characteristic energy E_0 corresponding to different (v_{th} , v_b) pairs.
- We can constrain the possible (v_{th} , v_b) pairs by specifying that E_0 should be less than 2 eV
- We find that

$v_{th} < 3.5$ km/s and thus

$v_b < 2$ km/s

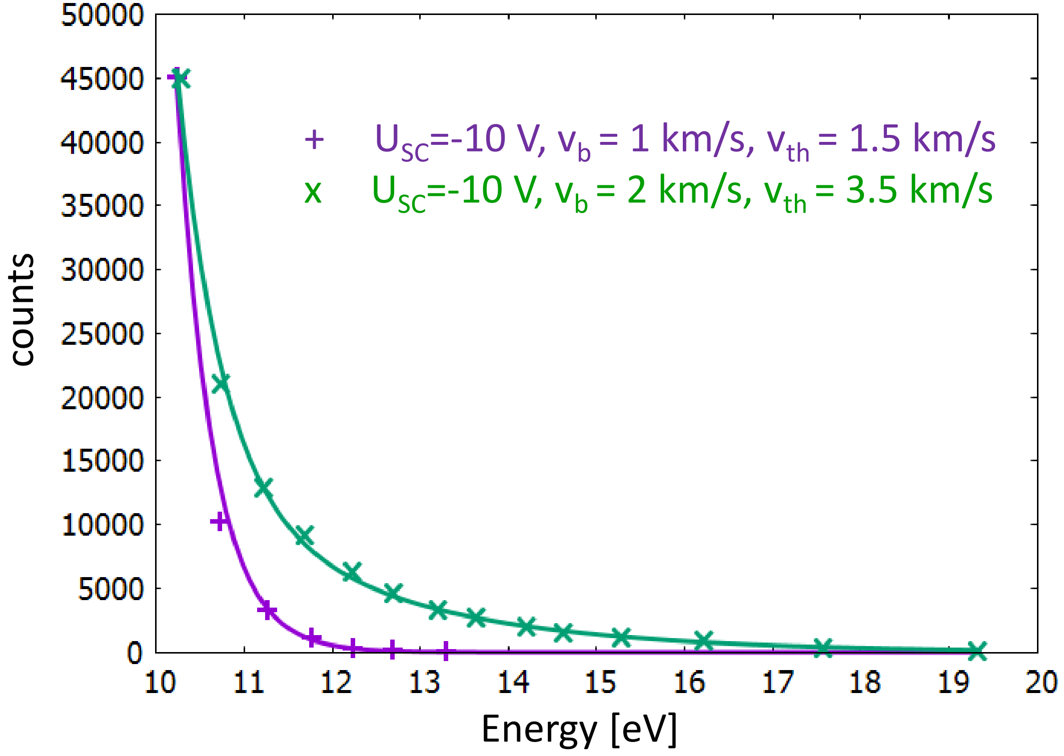

Conclusions

- The plasma is warm ($v_{th}/v_b > 1$)
- The v_{th}/v_b ratio increases with the bulk speed
- $v_{th} < 3.5$ km/s
- $v_b < 2$ km/s
- The low energy resolution during the investigated time intervals and the fast variation of the spacecraft potential prevents a more precise upper limit. It is possible that the speeds are significantly lower than the above values, but the data is inconsistent with higher bulk and thermal speeds.

References

- Bergman et al., JGR (2020) doi:1029/2019JA027478
- Goldstein, R., et al., GRL (2015) doi:10.1002/2015GL063939.
- Odelstad et al, MNRAS (2017) doi:10.1093/mnras/stx2232
- Stenberg Wieser et al, MNRAS (2017) doi:10.1093/mnras/stx2133

- Stenberg Wieser et al, EGU2020-8318